Eur. Phys. J. B **51**, 87–99 (2006)
DOI: 10.1140/epjb/e2006-00192-y

THE EUROPEAN PHYSICAL JOURNAL B

Nonlinear excitations and electric transport in dissipative Morse-Toda lattices

A.P. Chetverikov[1,2,a], W. Ebeling[1,3,b], and M.G. Velarde[1,c]

[1] Instituto Pluridisciplinar, Universidad Complutense, Paseo Juan XXIII, 1, 28040 Madrid, Spain
[2] Faculty of Physics, Saratov State University, Astrakhanskaya 83, 410012 Saratov, Russia
[3] Institut für Physik, Humboldt-Universität Berlin, Newtonstr. 15, 12489 Berlin, Germany

Received 18 October 2005 / Received in final form 17 January 2006
Published online 31 May 2006 –

Abstract. We investigate the onset and maintenance of nonlinear soliton-like excitations in chains of atoms with Morse interactions at rather high densities, where the exponential repulsion dominates. First we discuss the atomic interactions and approximate the Morse potential by an effective Toda potential with adapted density-dependent parameters. Then we study several mechanisms to generate and stabilize the soliton-like excitations: (i) External forcing: we shake the masses periodically, mimicking a piezoelectric-like excitation, and delay subsequent damping by thermal excitation; (ii) heating, quenching and *active* friction: we heat up the system to a relatively high temperature Gaussian distribution, then quench to a low temperature, and subsequently stabilize by *active* friction. Finally, we assume that the atoms in the chain are ionized with free electrons able to move along the lattice. We show that the nonlinear soliton-like excitations running on the chain interact with the electrons. They influence their motion in the presence of an external field creating dynamic bound states ("solectrons", etc.). We show that these bound states can move very fast and create extra current. The soliton-induced contribution to the current is constant, field-independent for a significant range of values when approaching the zero-field value.

PACS. 05.70.Fh Phase transitions: general studies – 05.40.Jc Brownian motion – 05.70.Ln. Nonequilibrium and irreversible thermodynamics

1 Introduction

Recently, we have developed the statistical thermodynamics of one-dimensional (1D) lattices with Morse interactions [1–4]. In particular we have investigated the clustering problem in low density 1D Morse lattices. A cluster was defined as a maximum of the local density, which is stable with respect to collisions. In the present report we concentrate on the opposite case of higher densities where the exponential repulsion dominates. The features of high-density Morse lattice rings has already been investigated in earlier work, where we could identify phonon peaks as well as peaks corresponding to solitonic excitations [3]. At relatively high densities the equilibrium clusters created by the attractive part of the forces become unstable due to the strong repulsion at small distances. We consider a system as dense, if the average distance between particles is equal or less than the distance where the potential minimum is located. We shall show, that in such dense systems excitations exist, which are soliton-like, whose generation and evolution along the lattice we study. Further, we discuss the influence of soliton-like excitations on electric transport. In recent communications the authors have already predicted [5] and discussed [6,7], albeit in a sketchy way, the possibility of soliton-mediated electric conduction in nonlinear lattices. Here we thoroughly study the influence of nonlinear interactions in dense Morse chains on electron dynamics and electric transport. We will make use of the fact that dense Morse chains may be well approximated by effective Toda chains with density-dependent adapted potential parameters. For illustration, the parameters of the forces used in this work are chosen in a range typical for hydrogen bonded polypeptide chains, such as α-helices [8–13]. Although our model-problem is a 1D-lattice we think that understanding the equilibrium, dynamic and transport features of 1D systems has always proven useful [14–18] for the subsequent work in 2D and 3D cases.

2 The Morse potential and other models of atomic interaction with exponential repulsion

The Morse potential was introduced in 1929 by Morse in a paper with the title "Diatomic molecules according

[a] e-mail: chetverikovAP@info.sgu.ru
[b] e-mail: ebeling@physik.hu-berlin.de
[c] e-mail: mvelarde@pluri.ucm.es

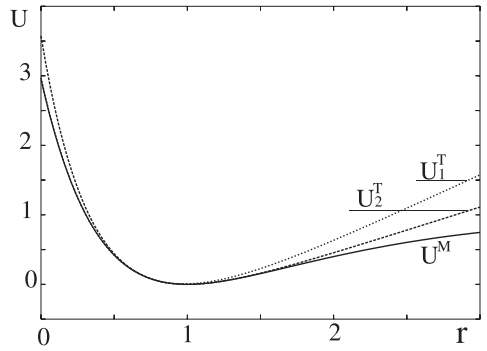

Fig. 1. Morse potential $B = D = 1; \sigma = 1$ (U^M, solid line), and effective (equivalent) Toda potential (U_1^T, upper dotted line) adapted to the minimum at $r_0 = \sigma$ ($a = 2/3; b = 3$). The third curve (U_2^T, lower dotted line) gives the effective Toda potential adapted to the point $r_0 = \sigma/2$ and therefore corresponding to twice higher density. In this case the effective Toda potential is nearly identical with the Morse case left to the minimum, but is higher on its right.

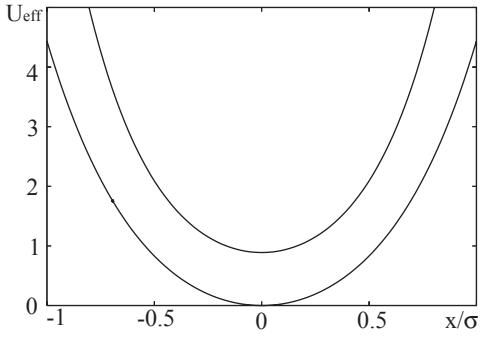

Fig. 2. Effective Morse potential (solid line) acting on a given particle placed between two other Morse particles at distance 2σ with $D = B = 1$. We compare with the corresponding result obtained from an effective Toda potential (dotted line) with the adapted parameters $a = 2/3$, $b = 3$.

to wave mechanics" [19]. Morse treated the problem of atomic interactions at small distances and derived a simple expression for the quantum interactions between atoms. The potential depends on two parameters B, D and reads

$$U^M(r) = D(\exp(-B(r-\sigma)) - 1)^2. \tag{1}$$

The potential has a minimum at $r = \sigma$ and may be considered as a good alternative to the Lennard-Jones model [7,20,21]

$$U^{L-J}(r) = \frac{B}{r^{12}} - \frac{A}{r^6}. \tag{2}$$

The long range part of the Morse potential is less realistic than the $1/r^6$ term in the Lennard-Jones potential. However the exponential repulsion term in the Morse potential has solid quantum-mechanical foundations. The predominant cause of exponential repulsion between atoms is the overlapping of wave functions of the valence electrons and is created mostly in the region close to the axis between the atoms [22].

The repulsive part of the Morse potential is similar to the repulsive part of the Toda potential

$$U^T(r) = \frac{a}{b}\left[\exp(-b(r-\sigma)) - 1 + b(r-\sigma)\right]. \tag{3}$$

Toda [16] found analytical solutions describing the nonlinear excitations in 1D lattices with equation (3) as interaction. The linear frequency connected with the Toda potential is

$$\omega_0^2 = \frac{ab}{m},$$

where m is the mass of the particles. Since the Toda potential is exactly solvable, it seems useful to approximate the Morse potential with the parameters B and D by a Toda potential. In the region around the minimum a useful approximation of the Morse potential by an effective Toda potential is obtained with the choice

$$a_{\mathit{eff}} = a = \frac{2}{3}BD, \qquad b_{\mathit{eff}} = b = 3B. \tag{4}$$

With this choice the Morse potential $U^M(r)$ and the effective Toda potential U_{eff}^T have nearly identical shape around the minimum, as shown in Figure 1. This is due to the fact that the Taylor expansions around the minimum are identical up to the third order and the fourth orders are very near to each other. Our approximation by an effective Toda potential is done to help us finding approximate analytical solutions for systems where the mean distance between particles corresponds to the minimum:

$$r_0 = \frac{L}{N} = \frac{1}{n} = \sigma, \tag{5}$$

(L is the length of the elementary cell which serves as the element for periodic repetition, N is the number of particles in a cell).

We shall study now the forces acting on a single particle embedded into a 1D lattice. Take a Morse particle placed midway between two other nearest-neighbor Morse particles separated by the average distance $2r_0$. Clearly, the inner particle is bound to experience quasilinear oscillations around the minimum for small excitations and nonlinear oscillations with large elongations due to the anharmonicity of equation (1). If the displacement from the center is denoted by x, the effective embedding potential felt by the central particle is (see Fig. 2)

$$U_{em}^M = 2D[\exp(2B(\sigma - r_0))\cosh(2Bx) - 2\exp(B(\sigma - r_0))\cosh(Bx)]. \tag{6}$$

We see from Figure 2, which corresponds to the equilibrium density (5), $r_0 = \sigma$, that an effective Toda potential with adapted parameters $a = (2/3)DB, b = 3B$ is nearly identical in shape with the result obtained for the Morse potential. For higher densities ($r_0 < \sigma$) the particles do not oscillate around the minimum but move in average on the repulsive branch of the Morse potential, left to the

minimum. In this case the effective oscillation frequency is given by the second derivative of the Morse potential at $r = r_0$:

$$m\omega_0^2 = U''^M(r = r_0) = 4B^2D\left[\exp(2B(\sigma - r_0) - \frac{1}{2}\exp(B(\sigma - r_0)\right]. \quad (7)$$

Then we can write a useful approximation by a Toda-type potential which at $r = r_0$ is adapted to the Morse potential:

$$U^T(r) = U^M(r_0) + U'^M(r_0)(r - r_0) + \frac{m\omega_0^2}{b_0^2}\left[\exp(-b_0(r - r_0)) - 1 + b_0(r - r_0)\right], \quad (8)$$

with density-dependent parameters (for simplicity we omit in the following the argument r_0). The dash denotes derivative. The stiffness parameter b_0 may be used to fit the third derivative

$$b_0 = \frac{U'''^M(r_0)}{U''^M(r_0)} = \frac{U'''^M(r_0)}{m\omega_0^2}, \quad (9)$$

so that

$$b_0 = 2B\frac{1 - \frac{1}{4}\exp(-B(\sigma - r_0))}{1 - \frac{1}{2}\exp(-B(\sigma - r_0))}.$$

Please note that our choice of the effective parameters introduces an implicit density dependence of the effective Toda potential. The effective Toda potential (8) is also called the local Toda approximation to the Morse potential. Note also that the constant and the linear terms in equation (8) are irrelevant, the constant term gives no contribution to the forces and the linear terms cancel in systems with periodic boundary conditions. The embedding potential (expressed by the equivalent local Toda approximation) has for high densities (5), $r_0 \ll \sigma$, a similar form as shown in Figure 2 for the case $r_0 = \sigma$,

$$U_{em}(x) = 2\frac{m\omega_0^2}{b_0^2}\exp(b_0(\sigma - r_0))\cosh(b_0 x). \quad (10)$$

In particular this approximation provides the correct oscillation frequency ω_0 of the central particle.

There are other possible potentials with exponential repulsion. A useful combination between the Toda- and the Lennard-Jones potentials is the Buckingham (exp6) potential that describes well (with appropriate parameters) realistic cases

$$U^B(r) = A\exp(-b(r - \sigma)) - B\left(\frac{\sigma}{r}\right)^6. \quad (11)$$

Since computer simulations with an r^{-6}-tail may give rise to numerical difficulties (due to its long range often avoided by setting a cut-off at some finite distance) we prefer here to work with the Morse potential which has an exponentially decaying attractive tail. A different way to treat the Buckingham potential is an approximation by an effective Toda potential, fitting as for the Morse case, the height and the first three derivatives at $r = r_0$. Let us emphasize that these potential models with exponential repulsion are quite realistic for the description of dense systems, where the Pauli repulsion between the overlapping valence shells of the atoms dominates.

Using effective Toda potentials facilitates not only the computer simulations but also the thermodynamic calculations, since one may use standard formulae developed for the thermodynamics of Toda potentials [23,24]. In particular, we shall be studying nonlinear excitations and their possible influence on electric transport, e.g., the coupling between nonlinear excitations and electric charges in ionized Morse chains. For illustration, the parameter values of the Morse potential will be chosen in a range typical for hydrogen bonded polypeptide chains [8–13].

3 Nonlinear dynamics of Morse and equivalent 1D Toda lattices

Let us first consider a 1D Toda and 1D Morse lattices consisting of N equal atoms (mass, m) with periodic boundary conditions disregarding ionization. Let us assume that the mean distance between the particles is $r_0 = L/N = \sigma$ where L and N are, respectively, the length and the number of particles in the chain (5). The particles are described by coordinates $x_j(t)$ and velocities $v_j(t)$, $j = 1, \ldots, N$. Note that $r_0 < \sigma$ may be reached only by applying external pressure.

In the presence of random forces (hence non zero temperature) and also external forces the dynamics is described by the Langevin equations

$$\frac{d}{dt}v_j + \gamma_0 v_j + \frac{1}{m}\frac{\partial U}{\partial x_j} = \frac{1}{m}F_j(x_j, v_j)) + \sqrt{2D_v}\,\xi_j(t), \quad (12)$$

governing the stochastic motion of the jth particle on the lattice. The stochastic forces $\sqrt{2D_v}\,\xi_j(t)$ model a surrounding heat bath (Gaussian white noise). The term γ_0 describes the standard friction frequency acting equally on all the atoms in the chain from the side of the surrounding heat bath. The validity of an Einstein relation is assumed [1]

$$D_v = k_B T\gamma_0/m, \quad (13)$$

where T is the temperature of the heat bath. Note that in non-equilibrium there exist several other temperature concepts [4]. The force F_j acting on the particles may include external driving as well as interactions with host particles (like electrons as we shall consider further below) embedded into the lattice.

The potential energy stored in the ring reads

$$U = \sum_{j=1}^{N} U(x_j). \quad (14)$$

First we will study the basic excitations when $F_j = 0, \gamma_0 = 0, D_v = 0$. For illustration, we shall consider a linear chain

of $N = 10$ atoms located on a ring; this is equivalent to a chain with periodic boundary conditions:

$$x_{j+N} = x_j + L. \tag{15}$$

Assuming that the mean distance (5) of the particles r_0 is near to the equilibrium distance r_{min} we may linearize the potential, hence approximating (10) by linear springs. Using the deviations from it $r_j = x_{j+1} - x_j - r_{min}$ (relative mutual displacements) we find in the case of small amplitudes

$$U(r_j) = \frac{m}{2}\omega_0^2 r_j^2,$$

corresponding indeed to a harmonic pair interaction potential. For N masses connected by linear springs, noise-free, and frictionless we get the following linear system of equations for the displacements u_j from equilibrium positions:

$$\frac{d^2}{dt^2}u_j + \omega_0^2\left(u_{j+1} + u_{j-1} - 2u_j\right) = 0.$$

The basic solution of this system reads

$$u_j^{(n)}(t) = A\cos(\omega_n t - jk_n\sigma). \tag{16}$$

There exist N different excitations corresponding to different wave lengths and corresponding wave numbers

$$-\frac{N}{2} < n \leq +\frac{N}{2}, \tag{17}$$

or wave "vectors" $k_n = 2\pi n/N\sigma$,

$$-\frac{\pi}{\sigma} < \frac{2\pi n}{N\sigma} \leq +\frac{\pi}{\sigma}. \tag{18}$$

This is the so-called Brillouin zone [25]. Recall that k-values in the region $k \pm \frac{2\pi}{\sigma}$ are equivalent due to the 2π-periodicity of the $\cos(x)$. The spectrum of eigen frequencies corresponding to linear collective vibrations, which are the phonons, is

$$\omega_n = \pm 2\omega_0 \sin\left(\frac{\sigma}{2}k_n\right). \tag{19}$$

This is also called the *acoustical* branch. The frequency increases with the modulus of the k-value. A special role play in our case ($N = 10$) the slow mode with $n = \pm 1$ and the fast *optical-like* mode $n = \pm 5$.

The phonon modes were obtained by linearization of the equations of motion. Let us see now the anharmonic case. We have shown that in the case of high densities, $r_0 \leq \sigma$, the Morse chain is determined by the exponential repulsion of the particles and can be approximated by an equivalent adapted Toda lattice. Accordingly, the Morse chain may be approximated by a chain of N point masses m interacting with Toda forces with adapted density-dependent parameters $\omega_0(r_0), b(r_0)$. The uniform Toda lattice possesses solutions representing cnoidal waves and soliton-type solutions [16]. Soliton solutions represent stable local excitations. They generate local energy spots which are running along the lattice. For a uniform chain, Toda found the following exact integrals of the Hamiltonian equations [16].

$$\exp\left(-b(r_{j+1} - r_j)\right) = const Z(2K(k))Z\left(\omega_0 t \pm jk\right). \tag{20}$$

Here $Z(u), K(k)$ represent elliptic integrals and elliptic functions respectively. (For simplicity we assume here units such that $r_0 = \sigma = 1$.) By adjusting appropriately the periodic boundary conditions for the N particles we find N *normal* modes, which are the nonlinear generalizations of the phonon modes found before for the harmonic potential. For the special case of an infinite lattice, $N \to \infty$, one of the solutions reduces to

$$\exp\left(-b(r_{j+1} - r_j)\right) = 1 + \sinh^2(\chi)\mathrm{sech}^2\left(\chi j - t/\tau\right). \tag{21}$$

These solitonic excitations correspond to local compressions of the lattice with the characteristic compression time

$$\tau_{sol} = \left(\omega_0 \sinh\chi\right)^{-1}, \tag{22}$$

and with the spatial "width" χ^{-1}. This quantity is connected with the energy of the soliton by

$$E^{sol} = 2\epsilon(\sinh\chi\cosh\chi - \chi). \tag{23}$$

As the energy unit we shall take the energy of an oscillator with frequency ω_0 and amplitude σ:

$$\epsilon = m\omega_0^2\sigma^2. \tag{24}$$

Toda's solution (21) represents a compression wave running along the chain. In the following we shall use the function

$$\begin{aligned} C_j(t) &= \exp[-b(r_j - r_{j-1})] - 1 \\ &= \exp[-b(x_{j+1} - 2x_j + x_{j-1})] - 1, \end{aligned} \tag{25}$$

to characterize the local strength of the solitonic pulse at site j.

For ideal Toda solitons

$$C_j(t) = \sinh^2(\chi)\mathrm{sech}^2\left(\chi(j-1) - t/\tau\right). \tag{26}$$

Due to its Hamiltonian structure the soliton energy is determined only by the initial conditions and such a soliton in a conservative lattice lives forever. For solitons in dissipative or forced Toda lattices we expect a soliton shape similar to a Toda soliton pulse (21). Further we expect, based on the possibility to approximate the Morse lattice by an adapted Toda lattice, that the essential solitonic features remain also valid for Morse lattices. This will be shown below. On the other hand, dissipation may lead to changes with respect to the conservative excitations, that we are going to study in detail. From now on we will distinguish between the cases of *weakly* dissipative solitons (with shape and velocity near to the conservative case) and *strongly* dissipative solitons (deviating albeit not too significantly from Eqs. (20–23)).

4 Excitation of soliton-like waves

4.1 Driving weakly dissipative solitons by external forcing

The solutions presented so far solve the Hamiltonian equations for Toda, and to some extent also for Morse lattices, in two limit cases, small and large amplitudes. Let us study now the generation of excitations in a weakly dissipative system including small friction and noise by forcing the elements. The aim is to force the masses $j = 1, ...\, N$ in such a way that the wanted excitations are generated. The forcing introduces energy into the system which in a stationary state has to be compensated by friction. We take the previous dynamical equations of Newtonian type, introduce friction forces and external spatial and time periodic forces. Then we have

$$\frac{d}{dt}x_j = v_j, \qquad j = 1, ...N,$$

$$m\frac{d}{dt}v_j = F_j(t) - \frac{\partial U}{\partial x_j} - m\gamma_0 v_j. \tag{27}$$

In the case of small motions around r_{min} we may linearize. In order to generate phonons (or even cnoidal waves as we do later on) of order n we may apply the forcing

$$F_j^{(n)}(t) = F_0 m\omega_0^2 \sigma \cos(\omega_{ex}t - jk_n\sigma + \phi), \tag{28}$$

with frequency ω_{ex} and amplitude F_0. As we will show, in general, the value of the frequency for excitation should be a little bit higher than the value predicted by the dispersion relation for the linear case $\omega_{ex} \geq \omega_n$.

The physical realization of such a forcing is not simple. We may think about a piezoelectric material in which the chain is embedded, a kind of "waveguide". In this "waveguide" we may induce running excitations of a chosen type with given k_n and corresponding (adapted) ω_{ex}, which by a suitable device or coupling are transferred to the chain. We first consider the case of small amplitudes and linearized equations. In this case the dispersion relation will be obeyed exactly, $\omega_{ex} = \omega_n$. It can be shown that the driven system possesses an attractor given by

$$x_j^{(n)}(t) = A_0 \cos(\omega_n t - jk_n\sigma + \Phi), \tag{29}$$

with stable amplitudes and phases. A similar procedure is expected to work also for cnoidal waves. However in this case the dispersion relation has to be found numerically.

The differential equations (27) have been integrated by means of a fourth-order Runge-Kutta algorithm adapted for solving stochastic problems [26]. We used $l_0 = \sigma$ as the length unit and $t_0 = 1/\omega_0$ as the time unit. Figure 3 shows the trajectories of a 10-particle adapted Toda lattice (periodic b.c.) with a running external forcing according to equation (28). The stiffness is $b = 2$, and the amplitude of the forcing is $F_0 = 0.15$, hence we are in the anharmonic regime. Being in the nonlinear regime, the dispersion relation (19) is no more valid. We expect for the solitonic

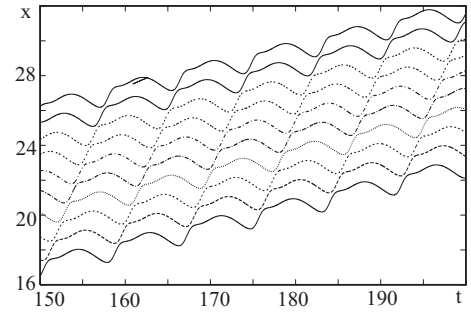

Fig. 3. Trajectories of $N = 10$ particles excited by an external force (28) $F_0 = 0.15, \omega_{ex} = 0.82$ in a *passive* Toda lattice with $b = 2, a = 1, \gamma_0 = 0.2$. One weakly dissipative soliton per unit cell is excited.

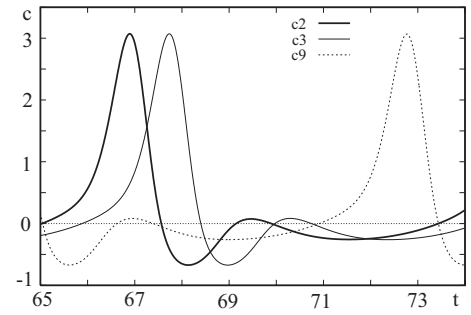

Fig. 4. The functions $C_j(t)$ (25) characterizing the soliton strength for the sites $j = 2, 3, 9$. The functions correspond to the forced soliton described in Figure 3.

mode a frequency $\omega_1 = 0.57$ and a velocity corresponding to the velocity of sound v_s ($v_s = 1$ in dimensionless units). In order to generate a solitonic mode we need a k-value corresponding to this mode. The frequency of the exciting wave should be somewhat higher than the value estimated from the dispersion relation for the linear case. The appropriate value for k which should be also used in the excitation wave is

$$k_1 = \frac{2\pi}{10\sigma} \simeq 0.628.$$

Then the corresponding appropriate frequency is $\omega_{ex} = 0.82$. In Figure 4 we depict the local shape of the soliton function $C_j(t)$ as defined above for the sites $j = 2, 3, 9$. We see that the pulse is indeed running along the lattice. The height of the pulse is a measure of the soliton strength which is determined here by the strength of the forcing. We see that the pulse has indeed a similar shape as Toda's soliton (26). In other words, the excitation created by the forcing remains soliton-like. At variance with Toda's function we observe that the forced excitation (Fig. 4) has a "tail", a kind of radiation due to the dissipation [27–29]. In Figure 5 we show for comparison a soliton excited under the same conditions in a Morse lattice. As we see, there is practically no significant difference. This is an important result, since the Toda lattice is more of academic interest, while the Morse lattice is able to model, with an appropriate choice on parameters, quite realistic situations, as e.g. with macromolecules [30].

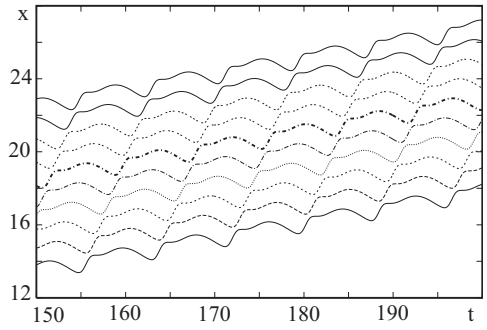

Fig. 5. Trajectories excited by an external forcing $F_0 = 0.5, \omega_{ex} = 0.82$ in a *passive* Morse lattice with $B = 1, \gamma_0 = 0.2$. The excited waves are qualitatively similar to those in a Toda lattice.

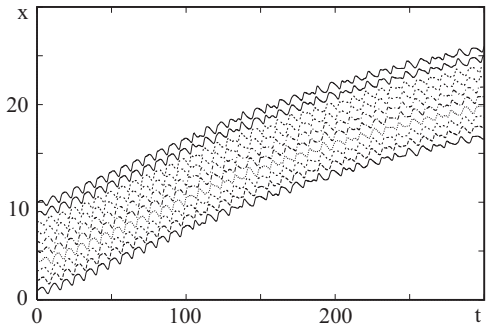

Fig. 6. Trajectories of $N = 10$ particles in a Morse lattice ($B = 1, \gamma_0 = 0.004$) excited by a external forcing $F_0 = 0.12, \omega_{ex} = 0.82$ which is switched off at time $t = 100$. We see that the excited soliton-like waves persist quite a long time after switching off the force ($F_0 = 0$ at $t > 100$) before they are damped out by friction.

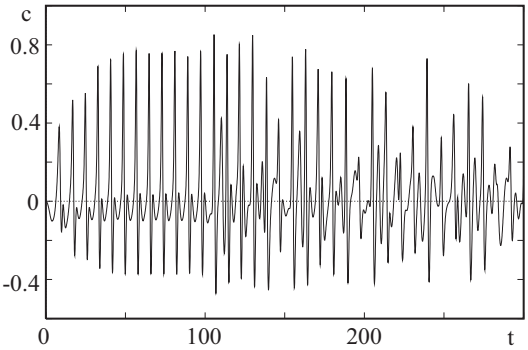

Fig. 7. The function $C_2(t)$ characterizing the soliton strength for excitations given in the previous figure.

We will study now a Morse lattice excited by an external force that we switch off after some time $t_{off} = 100$. Our choice for the friction is $\gamma_0 \simeq 0.004$, a value which seems to be realistic for hydrogen bonded polypeptide chains [8–13]. This value means that a linear oscillation is damped out after about 100 oscillations. Figures 6 and 7 show that after switching off the external driving force the solitonic modes persist for some time but also other modes appear. Upon increasing the damping, the relaxation time is decreasing as we see in Figure 8 for $\gamma_0 = 0.02, B = 1$.

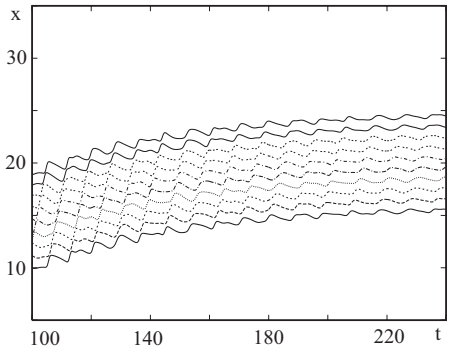

Fig. 8. Trajectories of $N = 10$ particles in an excited lattice for a higher value of damping than in Figures 6 and 7, $\gamma_0 = 0.02, B = 1$. We see that the excited soliton-like waves persist only a short time after switching off the force (forcing at $t < 100$). In a subsequent stage the solitons are first transformed to phonons before they are completely damped out by friction ($k_BT = 0$).

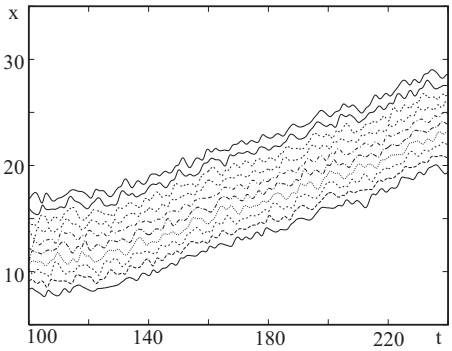

Fig. 9. The solitonic excitations given in the previous Figure 8 may be maintained by thermal fluctuations by embedding the lattice into a heat bath ($k_BT = 0.075$).

Switching on the noise by embedding the chain into a thermal heat bath, clearly increases the life time of the solitons as shown in Figure 9. We have chosen a temperature $k_BT = 0.075$, which is not too far from the critical temperature of the infinite lattice $k_BT_c \simeq 0.16$, where solitons are supported by thermal fluctuations [7,17,23,24,31]. Accordingly, solitonic excitations, which are quickly decaying in passive systems at $T = 0$, as we go up to the critical temperature become longer and longer lived metastable modes.

4.2 Excitation of strongly dissipative solitons by stochastic initial conditions and stabilization by active friction

Let us now consider a lattice without external forcing, $F_0 = 0$ (Fig. 10), using initial conditions created by a stochastic disturbance. We may think about sudden heating and quenching. We use a Gaussian distribution of the particle velocities corresponding to a relatively high-temperature Maxwellian as initial condition of the order of $k_BT_{in} \simeq 0.1$. Besides other excitations solitons are also generated. However they are difficult to recognize due to

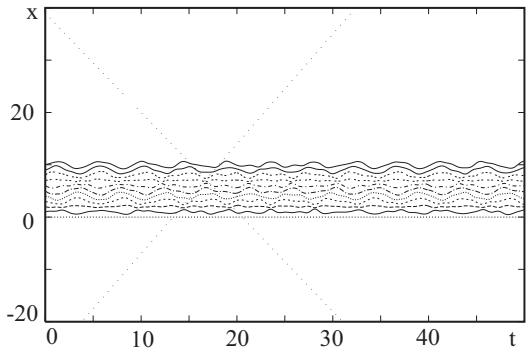

Fig. 10. Metastable cnoidal (solitonic) waves: As a result of quenching of an initial state with $k_BT \simeq 0.1$ the trajectories of 10 Toda particles ($r_0 = \sigma$) generate soliton-like excitations, which are represented by the slopes of the wavy trajectories.

the random motions of the particles. Then we quench to zero temperature. The solitons last longer since they have a longer lifetime than, with large space scale $\lambda \approx L$, most other excitations. Looking at the trajectories we observe the expected soliton-like excitations that decay after a time of the order $t_{rel} \simeq 1/\gamma_0$ (Fig. 10). These excitations exist also under equilibrium conditions [7,24]; they are metastable.

In order to maintain the solitonic excitations for quite a long time interval we apply an *active* friction in the time interval after heating and quenching. Then the soliton regime becomes a stable attractor [2,32–35]. A form of *active* friction is the velocity-dependent function

$$F(v) = m\gamma_0 v\left[\mu - v^2/v_d^2\right], \tag{30}$$

first introduced by Lord Rayleigh to maintain harmonic oscillations in the presence of dissipation [36,37] ($\mu = \delta - 1$, v_d appears as a parameter to set the velocity scale). Note that Lord Rayleigh's function differs from the later proposal by Van der Pol [38] of an *active* friction proportional to the space displacement (not the velocity) amplitude square. Then the quantity δ appears a *bifurcation* parameter. The value $\delta = 1$ corresponds to the passive case, where the deterministic dynamics has a single attractor at $v = 0$. Without noise all particles come to rest at $v = 0$. For $\delta > 1$ the branch $v = 0$ becomes unstable. There are two additional zeros at

$$v = \pm v_0 = v_d\sqrt{\delta - 1}, \tag{31}$$

which define the new attractors of the free deterministic motion if $\delta > 1$.

Recently, it was predicted [5] that electrons may be coupled to maintained solitons, using equation (30), and may form rather stable dynamic bound states with the solitons ("solectrons"). This effect is studied in detail in the next section (see also [39]).

5 Dynamics of electrons coupled to solitonic excitations

5.1 Models of electron dynamics

In order to study the possible influence of nonlinear excitations on electric transport we will assume now that the atoms can be ionized emitting one free electron to a kind of "band" and hence leaving a positive ion at the corresponding atom site along the lattice. This is like embedding N electrons between the N positive ionic masses on the chain. The interactions between the ions lattice will be described as above by a Toda potential with adapted parameters to mimic the Morse interactions. To describe the dynamics of the electrons we shall stay on a classical level as done in the early conductance theories of Drude, Lorentz and Debye [25,41]. Let us mention that the quantum treatment using the tight-binding approximation for the electron-(anharmonic) lattice vibrations does not qualitatively change the picture [8,9]. For discussion of related quantum problems see [10–13].

We take Langevin equations for N electrons (mass m_e, charge $-e$) and N ions (mass m, for all i, charge $+e$) moving on a lattice of length $L = N\sigma$, with $m_e \ll m$, with periodic boundary conditions. The N electrons are located at the positions y_l moving in the nonuniform, and, in general, time-dependent electric field generated by the positive lattice ion-particles located at x_j. The electron-electron interaction which results from Coulomb repulsion, Heisenberg uncertainty, and Pauli's exclusion principle, is modelled here in a rather crude way. We take into account that at small distances the effective potential is linear before it approaches at larger distances the classical Coulomb interaction [6]

$$U_{ee}(r) = U_{ee}(0) - \frac{e^2}{\lambda^2}r + O(r^2). \tag{32}$$

If the characteristic thermal wave length of the electrons

$$\lambda = \frac{\hbar}{\sqrt{m_e k_B T}},$$

is larger than the mean distance, we may use a piecewise linear approximation

$$\begin{aligned} U_{ee}(r) &= U_{ee}(0) - \frac{e^2}{\lambda^2}r \\ U_{ee}(r) &= 0 \qquad \text{if} \qquad r > \frac{U_{ee}(0)\lambda^2}{e^2}. \end{aligned} \tag{33}$$

This approximation leads to a rather weak constant repulsive force at small distances

$$F_{ee} = \frac{e^2}{\lambda^2} = \text{const.}, \tag{34}$$

which is much smaller than the purely classical Coulomb repulsion. The repulsive force F_{ee} acts between any pair of nearest-neighbor electrons and keeps them away from clustering. For degenerate electrons in 1D, the influence

of the repulsion is quite weak, since constant forces acting from right and from left on a given electron compensate each other. Hence for computational purposes the electron-electron repulsion will be neglected.

As done above the repulsive forces between ions are taken of exponential character. The additional Coulomb repulsion is of relevance only at relatively high densities. Therefore we may work again with an adapted local Toda approximation of type (8).

The electron-ion interaction will be described by a Coulomb potential with an appropriate cut-off as often used in plasma theory [6,41]

$$\epsilon_r U(r_{lj}) = (ee_j\kappa) - \frac{ee_j}{\sqrt{r_{lj}^2 + h^2}}, \tag{35}$$

if $r_{lj} < r_1$ and

$$\epsilon_r U(r_{lj}) = 0 \qquad \text{if} \qquad r_{lj} > r_1, \tag{36}$$

where $r_{lj} = y_l - x_j$ is the distance between the electron and its neighbors in the chain, e_j is the charge of the ion core of the chain particles. Further ϵ_r is the relative dielectric constant of the medium in which the chain is embedded, and $1/\kappa$ as well as r_1 play the role of appropriate "screening lengths". Here our choice is $r_1 = 3\sigma/4$, $\kappa = 2/\sigma$, and $\epsilon_r = 10$. We have introduced h as a parameter which determines the short-range cut-off of the Coulombic pole; an appropriate choice is $h \simeq 0.3\sigma$. Similar pseudo-potentials are of current use in solid state theory [25,42]. The choice of the concrete "depth" of the pole is made such that the electrons are only weakly bound to the ion cores and may cross from one side to the other of an ion. Accordingly, the electrons are able to wander through the lattice and, eventually, yield an electron current. The character of the electron dynamics strongly depends on the value of h and on the positions of the ions. Our choice $h \simeq 0.3\sigma$ provides two kinds of minima (see Figs. 11, 12): (i) shallow minima at the location of the ions outside a soliton pulse; and (ii) deep local minima at the positions of soliton-like pulses .

In correspondence to the dual structure of the potential landscape we have also a dual structure of the electron dynamics, hence the electrons may be divided roughly into two different classes:

$$N_e = N_e^f + N_e^b,\ N_e^f = \alpha N_e,\ N_e^b = (1-\alpha)N_e.$$

where α denotes the "degree of ionization". We have: (i) N_e^f free electrons that move like the free electrons in a plasma, or like the electrons in a conduction band in metals in a shallow periodic (harmonic) potential landscape; and (ii) N_e^b bound electrons that for a considerable time are pinned to one of the moving minima created by a solitonic excitation. This division is of course artificial. The essentially new point here is that there is the possibility of forming dynamic bound states ("solectrons") as predicted in reference [5]. The character of these bound states depends on the depth of the potential U_{min}, on the temperature T and on the relation between the characteristic *quantum* time $\tau_q \propto \hbar/U_{min}$ and the *classical* time scale

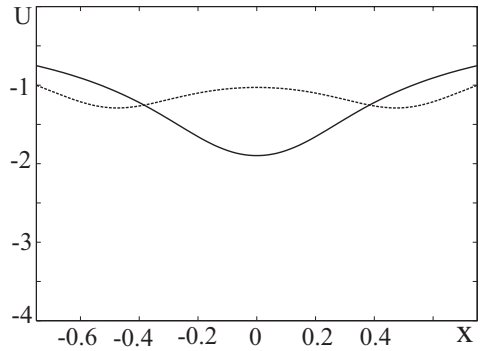

Fig. 11. Potential felt by an electron placed between two nearby positive ions at ±0.5 (abcissa: elongation in σ units). If the ions are at equilibrium distance, $r = \sigma$, the potential minimum is at the center of each ion core (dotted line). Between two compressed ions, $r = \sigma/5$, the potential minimum appears midway between the ions (solid line).

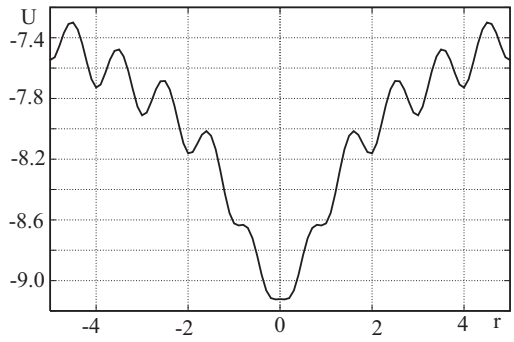

Fig. 12. Typical configuration of the local electric potential created by the solitonic excitation. The minimum corresponds to a local compression of ions which means an enhanced charge density.

$1/\omega_0$. Assuming that the classical time scales are much longer, we may take an adiabatic approximation [6]. Then the bound states are given by

$$\epsilon_n = U_{min} + \hbar\omega_{min}\left(n + \frac{1}{2}\right),$$
$$n = 0, 1, 2, ... \tag{37}$$

These states may, in principle, be filled by electrons obeying the Pauli principle. In the ground state, if enough number of solitons are available, each of the solitons can capture two electrons with opposite spin. At first glance, these electron pairs, which are Bosons, appear as kind of "bipolarons" or "Cooper pairs". We will come back to this point later. In a thermally excited but otherwise isolated system, the number of solitons does not depend on the initial and boundary conditions. Here the number of solitons can be approximated by the formula [17]

$$N_s = N\frac{\ln 2}{\pi^2}\frac{k_B T}{\epsilon}. \tag{38}$$

In principle the number of solitons increases with increasing temperature and may affect 2–5% of the number of

lattice sites around the critical temperature. This is a small but significant concentration of thermal solitons in the lattice. On the other hand their contribution to macroscopic properties, as e.g. the specific heat goes down as temperature increases. Therefore we will have in general a kind of "optimal temperature" where solitons have the strongest influence [3,7,17,23,24,31].

As a first approximation we may assume for the electron dynamics a classical "Drude-Lorentz-Debye dynamics" [5,6,25,30]

$$\frac{dv_l}{dt} + \frac{1}{m_e}\frac{\partial U_e}{\partial y_l} = -\gamma_{e0} v_l + \sqrt{2D_e}\,\xi_l(t) \qquad (39)$$

where γ_{e0} is connected to the relaxation time $\gamma_{e0} \propto 1/\tau$. Again, the stochastic forces $\sqrt{2D_e}\,\xi_l(t)$, model the surrounding heat bath (Gaussian white noise), obeying a fluctuation-dissipation theorem. Note that, due to the large difference in masses, the friction acting on the electron is small $m_e\gamma_{e0} \ll m\gamma_0$. The Drude-Lorentz-Debye model is not very realistic. However, it provides a model which can be easily treated by numerical simulations. It suffices to show, how the dynamical clusters created by solitonic excitations act on the electrons. A quantum-mechanical treatment of the electron dynamics within the tight-binding approximation has been given elsewhere [8,9]; it has been shown there, that the basic features described in the present work and in earlier works [5,6], are not significantly altered.

5.2 Influence of soliton modes on electron transport. Computer simulations

In order to study the coupling of electrons to the lattice vibrations we shall consider long trajectories of the electron positions and velocities, $v_l = \dot{y}_l$. Consider a Morse lattice in local Toda approximation, measuring the energy (temperature) in units $\epsilon = m\omega_0^2\sigma^2$ and fixing $b\sigma = 1$. Each electron is initially placed midway between two ions at rest, $v_l = 0$. As in the case earlier discussed, both differential equations (12) and (39) have been integrated by means of a fourth-order Runge-Kutta algorithm adapted for solving stochastic problems [26]. $l_0 = \sigma$ is the length unit and $t_0 = 1/\omega_0$ is the time unit.

The key parameter is the ratio between the strength of electric forces, which in average is of the order $e^2/\epsilon_r r_0^2$, and the strength of the lattice forces, being in average of order $m\omega_0^2 r_0$:

$$\eta = \frac{e^2}{m\omega_0^2\epsilon_r r_0^3}. \qquad (40)$$

In order to keep small the influence of the electrons, we take $\eta \simeq 0.01$. Since e is a universal constant, our choice means that we assume for the lattice frequency

$$\omega_0 = 10\left[\frac{e^2}{m\epsilon_r r_0^3}\right]^{1/2}. \qquad (41)$$

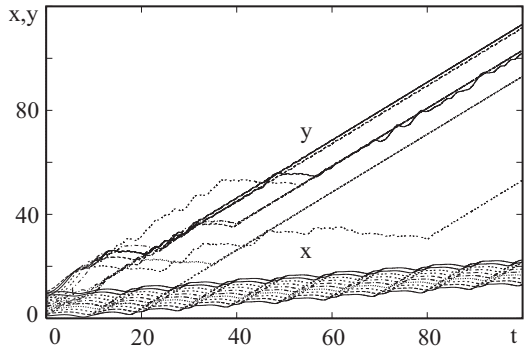

Fig. 13. Formation of "solectrons" and "solectron pairs": due to external forcing the trajectories of $N = 10$ positive ions (x, bottom part of figure) generate solitons. Several electrons are captured in solitonic potential wells (Fig. 12). During certain time intervals the electronic trajectories are parallel to the "tangents" representing the solitonic velocity. We observe free electrons (y), single "solectrons" and "solectron pairs" (Parameter values as in Fig. 3).

This is a rather high frequency which requires stiff springs. According to equation (7), in general this may be reached only by compression of the lattice, i.e., $r_0 < \sigma$.

In our first series of computer simulations the solitons were created by external forcing of the lattice. These solitons are *weakly* dissipative, the friction is small ($\gamma_0 \approx 0.2$). Looking at the trajectories displayed in Figure 13 we observe soliton-like excitations. The motions of ions and electrons occur in different time scales. Heavy ions are not much affected by the light electrons. Therefore the electrons move more or less adiabatically on the background of the Coulomb potential profile created by the ions. The dynamics of the ion ring leads to soliton-like excitations. As noted above, typical solitonic excitations correspond to local compressions moving along the lattice. Figure 12 shows a characteristic profile, a snapshot, of the electric field created by the ion ring at certain time instant. We see a rather deep potential well moving around the ring. The light electron may be captured in this dynamic potential well and eventually follows the soliton. In our simulations the integration step is chosen to describe correctly the fastest component of the process, the oscillations of electrons in the potential well.

Recall that with infinitesimal compressions the landscape would be purely harmonic (linear dynamics). With strong (local and moving) compressions the landscape is a composite made of cnoidal-like peaks upon a practically harmonic background. Due to such potential wells generated by the solitons, electronic bound states may be formed. In the course of time most of the electrons are captured in solitonic potential wells (see Fig. 13). During certain time intervals the electron trajectories are parallel to the "tangents" representing the solitonic velocity. We observe single "solectrons", also "solectron pairs" and multi-electron clusters.

In another series of computer experiments we excited *strongly* dissipative solitons maintained by *active*

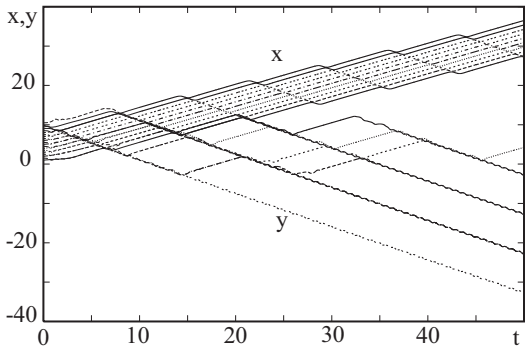

Fig. 14. Trajectories of 10 positive ions (x) moving clockwise creating one fast dissipative soliton moving in opposite direction to the motion of the ions, and trajectories of 10 electrons (y) captured in part by the soliton which is maintained due to the energy input by *active* friction ($\delta = 2$).

friction (30). Results are depicted in Figures 14 and 15. We used an initial Gaussian distribution of the ion velocities with amplitude v_{in} corresponding to an intermediate-temperature Maxwellian with $k_B T_{in} \simeq 0.1$ (as in earlier cases we use units of the energy of harmonic oscillations with amplitude σ). This is indeed in the soliton-generating region as $k_B T_c \simeq 0.16$ [3,7,17,23,24,31]. All computations start with an initial state of equal distances between ions. Such conditions may be reached experimentally by a suitable heat shock applied to the lattice. As besides other excitations many solitons are generated, we quenched to zero temperature.

As earlier done, in order to maintain the solitonic excitations for quite a long time interval we applied the *active* Rayleigh friction (30) in the period after heating and quenching. Then the soliton regime becomes a stable attractor [2,32–34]. In the driven case the ions perform a mean constant drift. After a transitory regime, solitonic excitations of the ions are formed moving along the lattice with velocity v_s opposite to the average drift of the ions. Most of the electrons are captured by these dynamical clusters. The computer simulations presented in Figures 14 and 15 correspond to Rayleigh friction (30) with $\delta = 2, v_d = 1, m/m_e = 1000, \gamma_0 = \gamma_{e0} = 0.2$. As the solitons corresponding to a local compression of the lattice are running opposite to the mean ion motion they, indeed, create a running potential well. Snapshots shown in Figures 14 and 15 illustrate how the electrons are captured in the running potential wells. Looking for the deepest nearby minimum of the potential, the electrons will be, most of the time, located near to local ion clouds. The soliton is a dynamic phenomenon, and the ions participating in the local compression are changing all the time. Hence, the electrons have always new partners for forming the "solectron", "solectron pairs" or higher-order clusters.

As said above, in the presence of *active* friction, the dynamical system possesses several attractors [2,32–34]. The computer simulations shown in Figure 14 correspond to initial conditions which lead preferentially to the single peak soliton attractor. In the absence of the external field

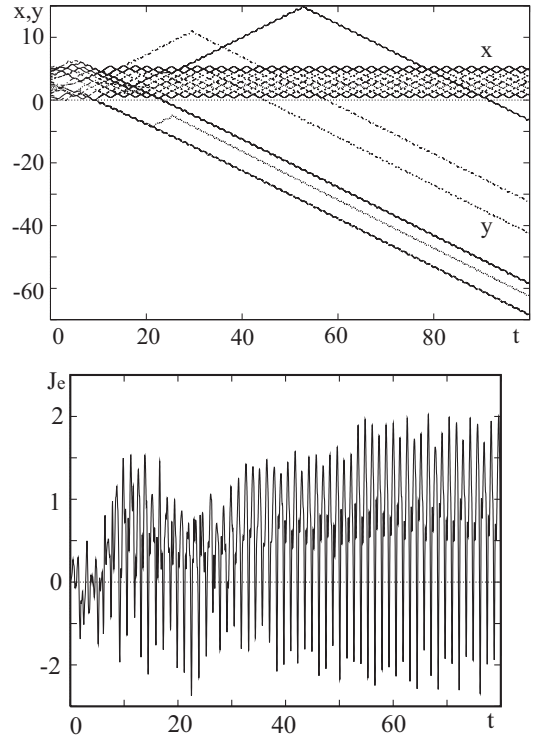

Fig. 15. Example of electrons (y) captured in the (nonlinear) optical-like mode. Due to random initial conditions and stabilization by active friction the trajectories of 10 positive ions (x) generate optical-like excitations (upper figure). The electrons may form bound states with local potential wells and perform forced oscillations. The lower figure shows the corresponding oscillatory current.

both directions have equal probability, the field breaks the symmetry. To simplify, the parameters of the potentials, of the Rayleigh formula, the friction coefficients, both masses and charges of particles were held fixed. The initial velocities v_{in}, the values of the external field and the (electron) temperature T_e (obtained from Einstein's relation obeyed by Eq. (39)) are varied in different runs.

In Figure 14 we show a computer simulation for the trajectories (left to right) of 10 ions creating a dissipative one-peak soliton which moves right to left. After a transient regime, the electrons are captured by solitons. By changing the initial conditions we have been able to excite the optical mode, where neighboring ions move always in counter phase. This mode is the driven nonlinear version of the optical oscillations in linear lattices. Figure 15 shows that this nonlinear mode is also able to capture electrons and force them to oscillate. Accordingly, the corresponding electron current is also oscillatory.

6 Influence of nonlinear excitations on the currents

The currents on the 1D ion-electron lattice, or line conductor, are determined by the electrons. The electron current density is given by averages of the electron velocities,

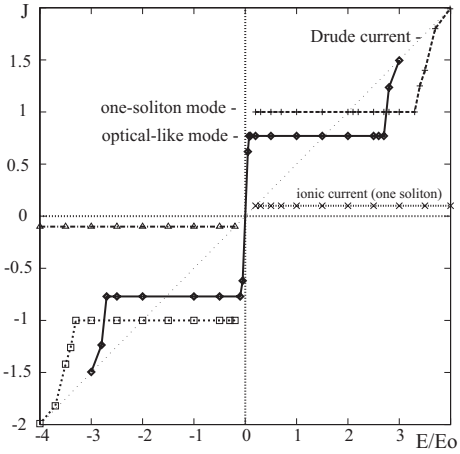

Fig. 16. Solectron and (positive) ion stationary currents in a lattice corresponding to the case of dissipative solitons maintained by *active* friction as functions of the field strength. (i) Currents for the single-peak soliton mode (parameter values: $b = 1, h = 0.3, \delta = 1.25, \gamma_0 = \gamma_{e0} = 0.45, D_v = 0$); (ii) currents for the optical mode (parameter values: $b = 2, h = 0.2, \delta = 2, \gamma_0 = \gamma_{e0} = 2.0, D_v = 0$). The dotted oblique straight line gives for comparison the linear Drude-Ohm current. It clearly appears that as we lower the field strength a transition occurs from linear to nonlinear hence non-Ohmic conduction. E_0 is the field strength creating the same force as the friction at velocity v_0 ($eE_0 = m\gamma_{e0}v_0$). Points above ($E > 0$) and below ($E < 0$) are marked differently to emphasize that the two branches have been calculated separately, and not plotted by symmetry.

$v_l = \dot{y}_l$ taken over long trajectories

$$j_e = -n_e e \sum_l \langle v_l \rangle. \tag{42}$$

An estimate of the electron currents may be based of the splitting given above. Treating the free electrons by standard theory [41] and taking into account that the bound electrons, the "solectrons" move (approximately) with soliton velocity we find the estimate (α denotes the fraction of free electrons)

$$j_e = \alpha \frac{n_e e^2}{m_e \gamma_{0e}} \pm (1 - \alpha) n_e e v_s, \tag{43}$$

which shows that the second contribution is independent of the external field. We expect therefore, that the currents are in (plateau-like) regions of "solectron formation" with $\alpha = 0$ constant.

In order to check these estimates we carried out several computer simulations. The results of computer simulations are displayed in Figure 16 for both the single-peak (one-soliton) soliton mode and the optical mode. The excitations were created by stochastic initial conditions with subsequent stabilization by *active* friction. Noteworthy is that the currents do not practically depend on the value of the field in a wide range of values, as expected from the estimate above. The characteristic value E_0 corresponds to the field imparting a velocity v_0 to an electron non interacting with ions. We see a strongly nonlinear current-field characteristics with a plateau region of constant current (corresponding to zero differential conductivity) as predicted in reference [5]. At very low, near zero field values there is a gap in values of the current. In the narrow region around zero field we could not find reliable data from the computer simulations. However the existence of a gap may be considered as a hint for the existence of rather high conductivity. In our computations too low a field value cannot specify the direction of motion for solitons, they may travel in either direction. On the other hand, too high a field value does not allow electrons to be trapped by a potential well, hence the current follows Drude-Ohm's law.

7 Discussion

We have shown that in 1D dense lattices of particles with exponential repulsion, soliton-like waves may be excited in the form of running local compressions. These dynamical clusters correspond to the cnoidal waves for a conservative Toda lattice (and also for a Morse lattice) [16]. We have shown, that these localized excitations may be generated also in dissipative lattices [27,28] by external forcing, or stochastic initial conditions, e.g., corresponding to a high enough heating observable by subsequent quenching. In order to measure the solitonic strength of the excitations, we used Toda's exponential function $C(t)$. Switching off the external excitation, the solitonic excitations survive only a finite time determined by the damping ($t_{rel} \propto 1/\gamma_0$); they are metastable. However, they may be maintained by means of an appropriate *active* friction included in the dynamics.

We have also studied the properties of ionized, hence electrically conducting lattices. Each atom was assumed to provide one electron moving along the chain in the field of the remaining ionic lattice. The electrons prefer positions near to the deep (electrostatic) potential well formed by the local compression connected with the soliton (see Figs. 11 and 12) thus creating a dynamic bound state, called solectron [5]. This solectron is to the anharmonic lattice what the polaron is to the harmonic case. Polarons are created by the polarization due to the electrical field of the electrons embedded into the lattice. Indeed, the electron attracts the neighboring ions by its electric field and gives rise to a local deformation/polarization of the lattice. The latter influences the electron by feedback effects and makes it to stay in some localized region of the lattice. On the other hand, the fast oscillations of the electron support the polarization. Our "solectrons" are due to the nonlinear dynamics of the lattice and, in particular, to the field created by the running solitonic excitations. The electrons are "slaved" to the anharmonic lattice excitations which act as true electric "carriers". Of course, the process of solectron formation is also connected with polarization effects. However, the latter are not the dominant effects. Let us insist that the dominant processes are in our case the autonomous, moving, anharmonic lattice excitations. Hence, solectrons are different from polarons in structure and, more important, in dynamics. Note that we study

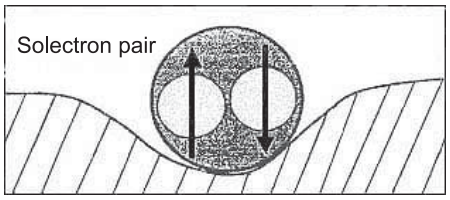

Fig. 17. Schematic picture of a "solectron pair": two electrons are bound together to a potential minimum created by a solitonic excitation.

here a single case, the one-way interaction electron-lattice vibration, which is expressed by the factor $\eta = 0.01$ which can be reached only by compressions in the lattice. The stronger the feedback of the electrons on the lattice is, e.g. at $\eta \simeq 1$, the more polaron effects we see.

We have shown with our computer simulations that under given conditions, formulated above, as time proceeds, if the soliton number is large enough, most of the electrons in the lattice are captured by solitonic excitations and move with the soliton velocity. Since the motion of solitonic excitations is slow with respect to the formation of quantum states, we expect the (adiabatic) formation of electronic quantum levels within the wells [6]. At each "location" two electrons with opposite spins may be placed, thus satisfying Pauli's exclusion principle. Indeed, if a sufficient number of strong solitons is available, then at least the ground state $n = 0$ may be populated. In the ground state two electrons may form pairs with opposite spins which populate a solitonic minimum as schematically illustrated in Figure 17. These pairs have bosonic character. At first glance these "solectron pairs" look like "bipolarons" or like "Cooper pairs" at low temperatures. A closer inspection however shows that the electron pairs created by solitonic excitations are quite different from bipolarons and from Cooper pairs: (i) on the one hand, the solectron pairs move most of the time with soliton velocity, which in general is supersonic in the lattice. Indeed, in our anharmonic system, strong compressions with hard repulsions provide a fast carrier wave along the lattice as predicted in reference [5]. Polarons are generally pinned in lattice sites, unless they extend over quite a large atomic domain; (ii) on the other hand, the dynamics of our solectron pairs is dissipative. Yet the amount of dissipation connected with the motion of the solectron pairs is low since the excited solitons are nearly those of the conservative limit (Toda lattice); (iii) the solectron pairs are not connected with any macroscopic wave functions, they are strictly local phenomena. The correlation length (the size) is small, much smaller than in the case of bipolarons and Cooper pairs; (iv) the correlation times of solitonic excitations and their bound states with electrons are large and the spectrum may exhibit $1/f$- contributions [5,23, 43]; (v) the formation of solectron pairs needs a source of excitation which can come either from external forcing or from a heat bath in some "optimal high temperature" [3, 7,17,23,24,31]).

Most of the results on electric conductivity presented here were obtained for the case of zero or very low temperature. The soliton carriers were created either by external forcing or by quenching and stabilized by *active* friction. In such systems, the number of solitons depends strictly on the initial and boundary conditions. However, there is a result (see Figs. 8 and 9) which shows the existence of long-living soliton modes in high temperature systems. This shows that solitons may be maintained also by appropriate thermal excitations. In principle the number of thermally excited solitons increases weakly with the temperature. On the other hand their stability and their contribution to macroscopic properties, as e.g. the specific heat goes down as temperature increases. Therefore we expect as in the case of specific heat [3,7,17,23,24,31]), the existence of a kind of "optimal high temperature" where solitons have the strongest influence on electric properties. This, however, remains an open question and will be the subject of future study.

Finally, in conclusion, we have shown how significant for electric conduction might be the role of bound states between dynamical solitons and electrons ("solectrons", etc.) thus confirming our earlier prediction [5]. Closely related dynamical phenomena, albeit for conservative systems, have been discussed by Zolotaryuk et al. [44] and by Hennig [45]. A full quantum theory of the phenomena described here is not available yet. First steps to a quantum approach in the framework of the tight-binding model have been given elsewhere [8,9].

The authors thank Dr. Valeri A. Makarov, Dr. Dirk Hennig, Dr. Jeff Porter, Dr. Christian Neiβner, Prof. Gregoire Nicolis, Prof. Gerd Röpke and Prof. Alwyn C. Scott, for enlightening discussions and correspondence. This research has been sponsored by the European Union under Grant SPARK, FP6-004690.

References

1. J. Dunkel, W. Ebeling, U. Erdmann, Eur. Phys. J. B **24**, 511 (2001)
2. J. Dunkel, W. Ebeling, U. Erdmann, V. Makarov, Int. J. Bifurcation Chaos **12**, 2359 (2002)
3. A.P. Chetverikov, J. Dunkel, Eur. Phys. J. B **35**, 239 (2003)
4. A.P. Chetverikov, W. Ebeling, M.G. Velarde, Eur. Phys. J. B **44**, 509 (2005)
5. M.G. Velarde, W. Ebeling, A.P. Chetverikov, Int. J. Bifurcation Chaos **15**, 245 (2005)
6. A.P. Chetverikov, W. Ebeling, M.G. Velarde, Contr. Plasma Phys. **45**, 275 (2005)
7. A.P. Chetverikov, W. Ebeling, M.G. Velarde, Int. J. Bifurcation Chaos **16**, in press (2006)
8. M.G. Velarde, W. Ebeling, D. Hennig, C. Neissner, Int. J. Bifurcation Chaos **16**, in press (2006)
9. D. Hennig, C. Neissner, M.G. Velarde, W. Ebeling, Phys. Rev. B **73**, 024306 (2006)
10. A.S. Davydov, *Solitons in Molecular Systems*, 2nd edn. (Reidel, Dordrecht, 1991)
11. A.C. Scott, Phys. Rep. **217**, 1 (1992)
12. D. Hennig, J.F.R. Archilla, J. Agarwal, Physica D **180**, 256 (2003)

13. D. Hennig, E.B. Starikov, J.F.R. Archilla, F. Palmero, J. Biol. Physics **30**, 227 (2004)
14. *Physics in One Dimension*, edited by J. Bernasconi, T. Schneider (Springer-Verlag, Berlin, 1981)
15. *The Many-Body Problem. An Encyclopedia of Exactly Solved Models in One Dimension*, edited by D.C. Mattis (World Scientific, Singapore, 1993)
16. M. Toda, *Nonlinear Waves and Solitons* (Kluwer, Dordrecht, 1983)
17. F.G. Mertens, B. Büttner, Mod. Problems Cond. Matter Phys. **17**, 723 (1986)
18. A.C. Scott, *Nonlinear Science. Emergence & Dynamics of Coherent Structures*, 2nd edn. (Oxford University Press, Oxford, 2003)
19. P. Morse, Phys. Rev. **34**, 57 (1929)
20. Ph. Choquard, *The Anharmonic Crystal* (Benjamin, New York, 1967)
21. R.S. Berry, B.M. Smirnov, Phys. Rev. B **71**, 144105 (2005)
22. M. Ross, F.H. Ree, J. Chem. Phys. **73**, 6146 (1980)
23. M. Jenssen, W. Ebeling, Physica D **141**, 117 (2000)
24. W. Ebeling, A. Chetverikov, M. Jenssen, Ukrain J. Phys. **45**, 479 (2000)
25. N. Ashcroft, N.D. Mermin, *Solid State Physics* (Holt, Rinehardt & Winston, Philadelphia, 1976)
26. N.N. Nikitin, V.D. Razevich, J. Comput. Math & Meth. Phys. **18**, 108 (1978)
27. V.I. Nekorkin, M.G. Velarde, *Synergetic Phenomena in Active Lattices, Patterns, Waves, Solitons, Chaos* (Springer-Verlag, Berlin, 2002)
28. C.I. Christov, M.G. Velarde, Physica D **86**, 323 (1995)
29. I.L. Kliakhandler, A.V. Porubov, M.G. Velarde, Phys. Rev. E **62**, 4959 (2000)
30. *Nonlinear Excitations in Biomolecules*, edited by M. Peyrard (Springer, Berlin, 1995)
31. M. Toda, N. Saitoh, J. Phys. Soc. Jpn **52**, 3703 (1983)
32. V. Makarov, W. Ebeling, M.G. Velarde, Int. J. Bifurcation Chaos **10**, 1075 (2000)
33. V. Makarov, E. del Rio, W. Ebeling, M.G. Velarde, Phys. Rev. E **64**, 036601 (2001)
34. E. del Rio, V.A. Makarov, M.G. Velarde, W. Ebeling, Phys. Rev. E **67**, 056208 (2003)
35. U. Erdmann, W. Ebeling, L. Schimansky-Geier, F. Schweitzer, Eur. Phys. J. B **15**, 105 (2000)
36. J.W. Strutt [Lord Rayleigh], Phil. Mag. **15**, 229 (1883)
37. J.W. Strutt [Lord Rayleigh], *The Theory of Sound* (Dover reprint, New York, 1941), Vol. I, Sect. 68a
38. B. Van der Pol, Phil. Mag **2** (Ser. 7), *ibidem*, **3** (Ser. 7), 65 (1927)
39. V.A. Makarov, M.G. Velarde, A.P. Chetverikov, W. Ebeling, Phys. Rev. E, in press (2006)
40. T. Pohl, U. Feudel, W. Ebeling, Phys. Rev. E **65**, 046228 (2002)
41. W. Ebeling, V.E. Fortov, Yu.L. Klimontovich, N.P. Kovalenko, W.D. Kraeft, Yu.E. Krasny, D. Kremp, P. Kulik, V.A. Riabii, G. Röpke, E. Rozanov, M. Schlanges, *Transport Properties of Dense Plasmas* (Birkhäuser, Boston, 1984)
42. V. Heine, M.L. Cohen, D. Weaire, *The Pseudopotential Concept* (Academic Press, New York, 1970)
43. Y.L. Klimontovich, *Statistical Physics of Open Systems* (Kluwer, Dordrecht, 1995)
44. A.V. Zolotaryuk, St. Pnevmaticos, A.V. Savin, Phys. Rev. Lett. **67**, 707 (1991)
45. D. Hennig, Phys. Rev. E **61**, 4550 (2000)